

SUPPLEMENTARY INFORMATION

Assessing the efficiency of water-soluble organic compounds biodegradation in clouds under various environmental conditions

Lucas Pailler^{1,}, Nolwenn Wirgot², Muriel Joly², Pascal Renard¹, Camille Mouchel-Vallon^{1,a}, Angelica Bianco¹, Maud Leriche¹, Martine Sancelme², Aurélie Job², Luc Patryl³, Patrick Armand³, Anne-Marie Delort², Nadine Chaumerliac¹, Laurent Deguillaume^{1,4,*}*

¹ Université Clermont Auvergne, CNRS Laboratoire de Météorologie Physique, F-63000 Clermont-Ferrand, France.

² Université Clermont Auvergne, CNRS, SIGMA Clermont, Institut de Chimie de Clermont-Ferrand, 63000 Clermont-Ferrand, France.

³ CEA, DAM, DIF, 91297 Arpajon, France.

⁴ Université Clermont Auvergne, CNRS, Observatoire de Physique du Globe de Clermont Ferrand, UMS 833, Clermont-Ferrand, France.

^a Now at: Laboratoire d'Aérodologie, Université de Toulouse, CNRS, UPS, Toulouse, France.

Correspondence: Laurent Deguillaume (laurent.deguillaume@uca.fr), Lucas Pallier (lucas.pailler@doctorant.uca.fr)

1- INCUBATION EXPERIMENTS

(S1) Bacteria growth conditions and cell concentration

Bacteria were grown in 10 mL of R2A medium (Reasoner and Geldreich, 1985) under agitation (200 r.p.m.) at 17°C for approximately 17 hours. Cells in exponential growth were collected by centrifugation for 3 min at 10481 xg. The supernatant was discarded, and the bacterial pellet was suspended and washed twice in the incubation medium (1X or 100X artificial cloud water). The concentration of cells was estimated by optical density measurement at 600 nm to obtain a concentration close to 10^7 cells mL⁻¹ for acetic acid and formaldehyde and 10^5 cells mL⁻¹ for hydrogen peroxide and formic acid studies. Thereafter, the concentration of cells was precisely determined by standard dilution-plating on R2A and incubation for 3 days at 17°C for CFU counts.

(S2) Artificial cloud solution

Bacteria were incubated in artificial cloud solution. This medium was prepared to mimic real cloud chemical composition representative of air masses influenced by marine emissions (Deguillaume et al., 2014). For formaldehyde and acetic acid, the artificial cloud solution was 100X concentrated as the bacteria were 100 times more concentrated than in cloud water. Stock solutions were prepared from ammonium nitrate (HNO₃ x H₂O; Fluka), magnesium chloride hexahydrate (MgCl₂ x 6H₂O; Sigma-Aldrich), potassium sulfate (K₂SO₄; Fluka), calcium chloride dihydrate (CaCl₂ x 2H₂O; Sigma-Aldrich), ammonium sulphate ((NH₄)₂SO₄; Fluka), sodium hydroxide (NaOH; Merck), sulphuric acid (H₂SO₄; Sigma-Aldrich).

Carbon compounds usually detected in cloud water (e.g. carboxylic acids and aldehydes) were not introduced so that the studied substrate was the only carbon source available for bacteria. Finally, the solution obtained was adjusted to pH 6 and sterilized by filtration (Polyethersulfone membrane, 0.22 µm; Fisher Scientific) before use.

Table SM1: Chemical composition of the artificial cloud solution.

Compound	Marine artificial cloud water	Cloud water classified as marine following Deguillaume et al. (2014)
Concentration (µM)		
Cl ⁻	24.0	25.3
NO ₃ ⁻	28.0	24.8
SO ₄ ²⁻	14.5	14.1
Na ⁺	14.0	25.7
NH ₄ ⁺	38.0	43.2
K ⁺	3.0	3.0
Mg ²⁺	4.0	3.9
Ca ²⁺	8.0	8.6
pH	6.0	5.7

(S3) Organic compounds and hydrogen peroxide H₂O₂ solutions

The biodegradation of four different chemical compounds were studied: formic and acetic acids, formaldehyde and hydrogen peroxide. Stock solutions were prepared from sodium formate and acetate salts (HCOONa, purity 99%, Sigma Aldrich; CH₃COONa, purity 99%, Sigma Aldrich,), from methanol-free formaldehyde solution (CH₂O, 16% (w/v); Thermo Fisher Scientific) and from a hydrogen peroxide solution (H₂O₂, 30%; not stabilized Fluka Analytical). The addition of a small volume of stock solution (X μ L) does not significantly modify the volume of the solution and the concentration of other species.

(S4) Chemical analysis

Formate and acetate concentrations were measured by ionic chromatography (Thermo ICS 5000+; column for anions: AS18; <10 A°; 13 μ M; 4x25 mm). The injected volume was fixed at 750 μ L with a flow rate of 0.25 mL/min. A binary mixture of potassium hydroxide and water was used as eluent. The separation was done by a gradient elution method (0 min: 0.2 mM; 4.5 min: 0.43 mM; 10 min: 5 mM; 13-14 min: 33.5 mM; 14.1 min: 0.2 mM). The uncertainty of measurement provided a level of confidence of approximately 94% for formate (calculated based on three replicates and four concentrations) and of approximately 90% for acetate (calculated based on three replicates and four concentrations).

The protocol used for formaldehyde quantification was adapted from Vander Heyden et al. (2002). In this protocol formaldehyde was derivatized in presence of 2,4-dinitrophenylhydrazine (2,4-DNPH) to form formaldehyde 2,4-dinitrophenylhydrazone. Briefly, 1 mL of incubation medium was spiked with 0.4 mL of 2,4-DNPH (0,1 %) and left for 5 minutes at room temperature. Products were stabilized by the addition of 0.4 mL of phosphate buffer (0.1 M, pH 6.8) and 0.7 mL of 1 M NaOH. Formaldehyde 2,4-dinitrophenylhydrazone was measured by high performance liquid chromatography (Dionex UV (UVD 340)) using a C18 column (100 A°; 5 μ m; 4.6 x 250 mm, Interchim Uptisphere Strategy) with a mixture of phosphate buffer (0.025 M, pH 4) and acetonitrile for the mobile phase (isocratic separation at 45/55 (v/v) phosphate buffer/acetonitrile). The uncertainty of measurement provided a level of confidence of approximately 93% (calculated based on three replicates and four different concentrations).

Fluorescence spectroscopy was used to quantify hydrogen peroxide concentrations (Safire II TECAN®; λ_{exc} = 320 nm, λ_{em} = 390 nm). A miniaturized assay based on a reaction between hydrogen peroxide, peroxidase (Horse Radish Peroxidase, HRP) and p-hydroxyphenylacetic acid (HPAA) was used (Lazrus et al., 1985; Vaitilingom et al., 2013). HPAA is oxidized by HRP, using H₂O₂ as an oxidizing agent and lead to the formation of a radical. The resulting radical is then subjected to a dimerization that forms a fluorescent dimer with concentration directly proportional to H₂O₂ content. The minimal value for the level of confidence is 92% (calculated based on five replicates and five different concentrations).

(S5) Incubation setup

Incubation experiments were conducted up to 24h in triplicates for two temperatures (17 and 5°C) and for different initial substrate concentrations. During each experiment, substrate concentrations were monitored with a shorter time step at the beginning of the incubation (8 first hours). This allows to calculate biodegradation rates (see S(6), below).

Control samples were analyzed to evaluate the substrate stability. One solution with substrate and no microorganisms allows to check if no degradation is observed during the experiment. Variations in substrate concentration do not exceed 5%. Other control samples with no substrate contain microorganisms to check if there is no substrate biological production. No production was observed during these experiments.

pH and cell concentrations were monitored at the beginning and end of the experiment and at 8h. As expected, at the end of the incubation time, we observed that the concentrations of microbial cells can slightly increase, and that the pH of the solution became more basic due to regulation by microorganisms.

(S6) Biodegradation rate calculation

The graphs representing the substrate concentration decrease as a function of time were plotted for all substrates (formic and acetic acids, formaldehyde, and hydrogen peroxide) and all experiments (various initial substrate concentrations and temperatures). Biodegradation rate (V_i) was determined for each substrate concentration as the maximal slope of the plot representing the concentration of substrate ($[S]$, in M) as a function of time (t , in s). V_i was then normalized by the cell concentration to obtain initial velocity expressed as mol per s per bacterial cell (*i.e.*, $\text{mol s}^{-1} \text{cell}^{-1}$).

Biodegradation rates for all experiments are summarized in Table SM2. The biodegradation rates errors were estimated by calculating standard deviations of the 3 biodegradation rates estimated from the 3 independent replicates.

Table SM2: Biodegradation rates for each chemical compound (formic acid, acetic acid, formaldehyde, H₂O₂) for concentrations of substrate and for two temperatures (5 and 17°C). The values were averaged from three replicates (except for formic acid experiments at 5°C done in duplicates) and standard deviations were calculated.

Compound (substrate)	Strain	Temperature (°C)	Substrate concentration (M)		Bacteria concentration (cell L ⁻¹)		Biodegradation rate x 10 ⁻¹⁹ (mol s ⁻¹ cell ⁻¹)
Formic acid	<i>Pseudomonas graminis</i> 13b-3	17	x 10 ⁻⁶	3.8 ± 0.2	x 10 ⁵	1.3 ± 0.6	20 ± 10
				6.08 ± 0.07		1.0 ± 0.1	70 ± 30
				11.2 ± 0.5		1.08 ± 0.08	140 ± 80
				22 ± 1		1.0 ± 0.2	340 ± 200
				52 ± 4		1.1 ± 0.3	950 ± 700
		5	x 10 ⁻⁶	3.9 ± 0.4	x 10 ⁵	2.1 ± 0.1	10.2 ± 0.4
				6.3 ± 0.2		1.2 ± 0.1	14 ± 4
				11.7 ± 0.2		1.5 ± 0.5	15 ± 4
				22.4 ± 0.6		1.0 ± 0.2	21 ± 2
				57.2 ± 0.4		1.20 ± 0.01	30 ± 20
Acetic acid	<i>Pseudomonas sp.</i> 14b-10	17 *	x 10 ⁻⁴	1.4 ± 0.2	x 10 ⁷	1.0 ± 0.9	11 ± 6
				2.8 ± 0.3		1.0 ± 0.5	12 ± 6
				4.5 ± 0.2		1.1 ± 0.5	11 ± 4
				7.7 ± 0.3		1.1 ± 0.6	11 ± 4
				10.4 ± 0.3		1.0 ± 0.7	10 ± 4
		5	x 10 ⁻⁴	28.6 ± 0.6	x 10 ⁵	2.1 ± 0.5	13 ± 2
				1.7 ± 0.7		1.3 ± 0.4	2.2 ± 0.8
				2.9 ± 0.6		1.0 ± 0.3	4 ± 1
				5.1 ± 0.5		1.2 ± 0.5	4 ± 2
				7.88 ± 0.09		1.0 ± 0.5	3.5 ± 0.7
Formaldehyde	<i>Pseudomonas syringae</i> 12b-8	17	x 10 ⁻⁴	0.26 ± 0.04	x 10 ⁷	1.4 ± 0.2	7 ± 3
				0.55 ± 0.06		1.6 ± 0.1	12 ± 4
				1.2 ± 0.1		1.5 ± 0.3	20 ± 10
				1.8 ± 0.2		2.0 ± 0.2	27 ± 15
				2.4 ± 0.3		1.6 ± 0.4	31 ± 15
		5	x 10 ⁻⁴	0.4 ± 0.2	x 10 ⁷	1.6 ± 0.3	4 ± 1
				0.8 ± 0.2		1.5 ± 0.2	8 ± 3
				1.6 ± 0.3		1.7 ± 0.2	17 ± 7
				2.4 ± 0.4		1.8 ± 0.4	15 ± 9
				3.2 ± 0.6		1.7 ± 0.7	30 ± 20
Hydrogen peroxide	<i>Pseudomonas graminis</i> 13b-3	17	x 10 ⁻⁴	0.026 ± 0.005	x 10 ⁵	1.5 ± 0.6	5 ± 3
				0.046 ± 0.007		1.7 ± 0.8	9 ± 7
				0.11 ± 0.01		1.5 ± 0.6	22 ± 15
				0.15 ± 0.02		1.3 ± 0.5	25 ± 25
				0.23 ± 0.03		1.4 ± 0.5	41 ± 40
				0.49 ± 0.06		1.4 ± 0.6	70 ± 10
				1.00 ± 0.06		1.5 ± 0.8	97 ± 4
		1.2 ± 0.2	1.8 ± 0.7	147 ± 3			
		5	x 10 ⁻⁴	0.023 ± 0.003	x 10 ⁵	1 ± 1	3 ± 2
				0.045 ± 0.002		1.1 ± 0.6	5 ± 3
				0.093 ± 0.009		1 ± 1	7 ± 4
				0.140 ± 0.006		1.2 ± 0.9	14 ± 8
				0.19 ± 0.03		0.9 ± 0.6	25 ± 10
				0.58 ± 0.03		1.6 ± 0.3	52 ± 7
1.07 ± 0.08	1.0 ± 0.6			82 ± 3			
1.45 ± 0.01	1.8 ± 0.7	90 ± 5					

* For acetic acid, one control (in grey) has been performed at cell concentration of 10⁵ cell L⁻¹, keeping the same cell/substrate ratio. This biodegradation rate is in the same range than the ones calculated with a 10⁷ cell L⁻¹ cell concentration.

2- MODEL SIMULATIONS

(S7) a) CLEPS aqueous phase mechanism

Tables are extracted from Mouchel-Vallon et al. (2017).

- Inorganic mechanism
→ Table-mechanism-inorganic-CLEPS.pdf
- Mechanism of organic compounds with one or two carbon atoms
→ Table-mechanism-C1-C2-CLEPS.pdf
- Mechanism of organic compounds with three carbon atoms
→ Table-mechanism-C3-CLEPS.pdf
- Mechanism of organic compounds with one or four carbon atoms
→ Table-mechanism-C4-CLEPS.pdf

(S7) b) Spinup parameters

Table SM3: a) Meteorological initial parameters and b) chemical scenarios used for the gas phase simulation.

		Summer case	Winter case		
Parameters					
Date of the simulation (beginning)		June 14 th	December 14 th		
Time of the simulation		8 days	8 days		
Temperature (K)		290	278		
Pressure (hPa)		860	860		
Relative humidity (%)		40	60		
Gas phase species	Initial mixing ratio (ppb)	Summer emission (molec cm ⁻³ s ⁻¹)	Summer deposition (s ⁻¹)	Winter emission (molec cm ⁻³ s ⁻¹)	Winter deposition (s ⁻¹)
SO ₂	0	6.0 10 ⁴	1.0 10 ⁻⁵	6.0 10 ⁴	7.0 10 ⁻⁶
NO	-	2.9 10 ⁵	-	2.9 10 ⁵	-
NO ₂	0.30	-	4.0 10 ⁻⁶	-	2.6 10 ⁻⁶
N ₂ O ₅	-	-	2.0 10 ⁻⁵	-	1.3 10 ⁻⁵
HNO ₃	0.30	-	2.0 10 ⁻⁵	-	1.3 10 ⁻⁵
O ₃	20	-	4.0 10 ⁻⁶	-	2.6 10 ⁻⁶
H ₂ O ₂	1.0	-	5.0 10 ⁻⁴	-	3.3 10 ⁻⁴
CH ₄	1.7 10 ³	-	-	-	-
CO ₂	3.6 10 ⁵	-	-	-	-
CO	0	3.7 10 ⁶	1.0 10 ⁻⁶	3.7 10 ⁶	7.0 10 ⁻⁷
Isoprene	1.0	5.0 10 ⁶ (a)	-	2.5 10 ⁶ (a)	-
Dihydroxybutanone	-	-	1.5 10 ⁻⁵	-	1.0 10 ⁻⁵
MACR	-	-	1.5 10 ⁻⁵	-	1.0 10 ⁻⁵
MVK	-	-	1.5 10 ⁻⁵	-	1.0 10 ⁻⁵
Glyoxal	0.10	-	1.5 10 ⁻⁵	-	1.0 10 ⁻⁵
Methylglyoxal	0.10	-	1.5 10 ⁻⁵	-	1.0 10 ⁻⁵
Glycolaldehyde	-	-	1.5 10 ⁻⁵	-	1.0 10 ⁻⁵
Acetaldehyde	0.10	3.2 10 ³	1.5 10 ⁻⁵	3.2 10 ³	1.0 10 ⁻⁵
Formaldehyde	0.10	1.0 10 ³	1.5 10 ⁻⁴	1.0 10 ³	1.0 10 ⁻⁴
Acetone	0.10	8.9 10 ³	1.5 10 ⁻⁵	8.9 10 ³	1.0 10 ⁻⁵
Pyruvic Acid	-	-	1.5 10 ⁻⁵	-	1.0 10 ⁻⁵
Acetic Acid	1.0 10 ⁻³	3.3 10 ³	1.5 10 ⁻⁵	3.3 10 ³	1.0 10 ⁻⁵
Formic Acid	-	-	1.5 10 ⁻⁵	-	1.0 10 ⁻⁵
Methanol	2.0	1.1 10 ⁴	1.5 10 ⁻⁵	1.1 10 ⁴	1.0 10 ⁻⁵
Methylhydroperoxide	1.0 10 ⁻²	3.3 10 ³	5.0 10 ⁻⁶	3.3 10 ³	3.3 10 ⁻⁶

(a) 0 at night-time concentration

(S7) c) Spinup gas phase concentrations

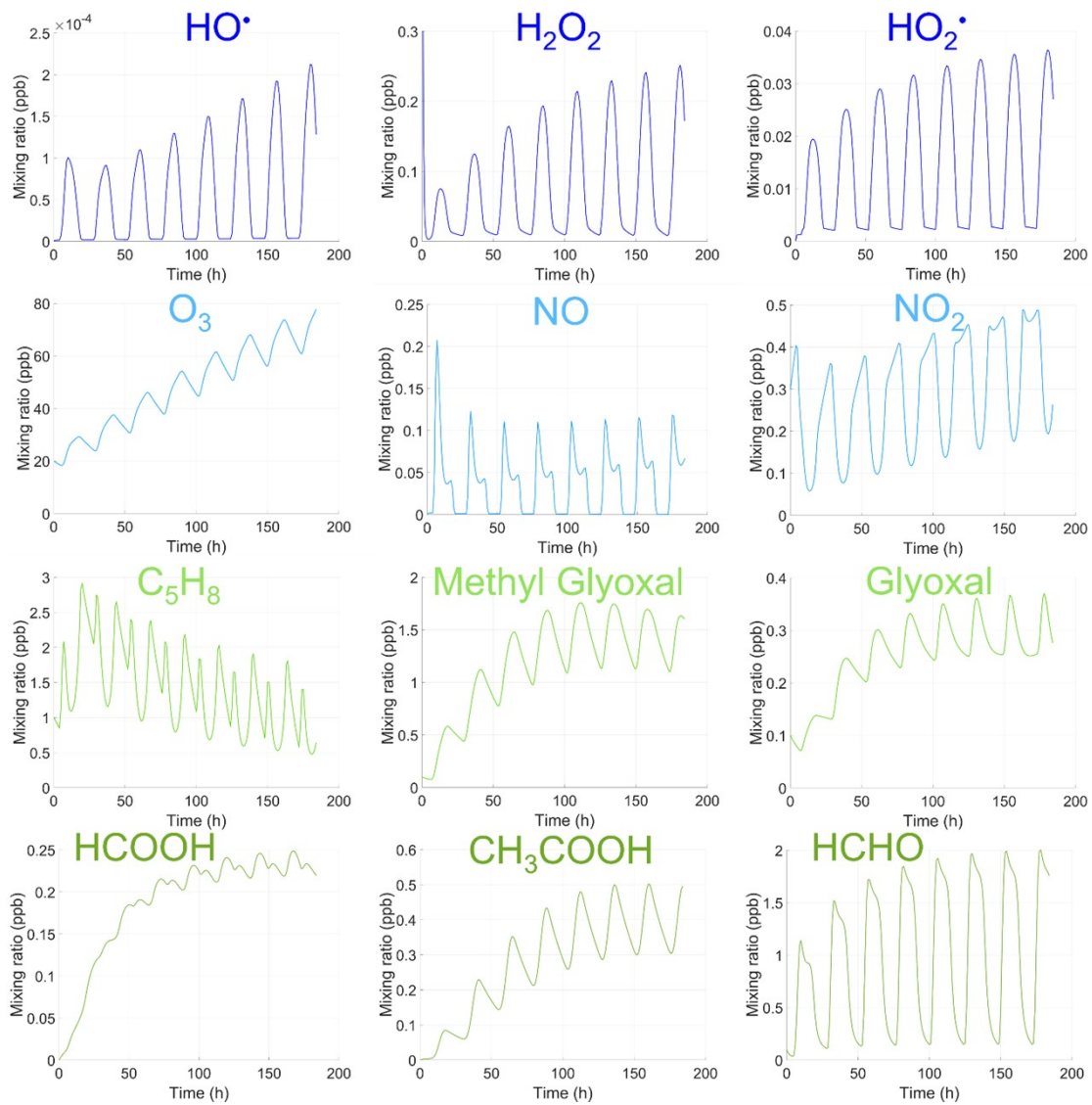


Figure SM1: Time evolution of the concentration (ppb) of some selected gases during the spinup summer simulation.

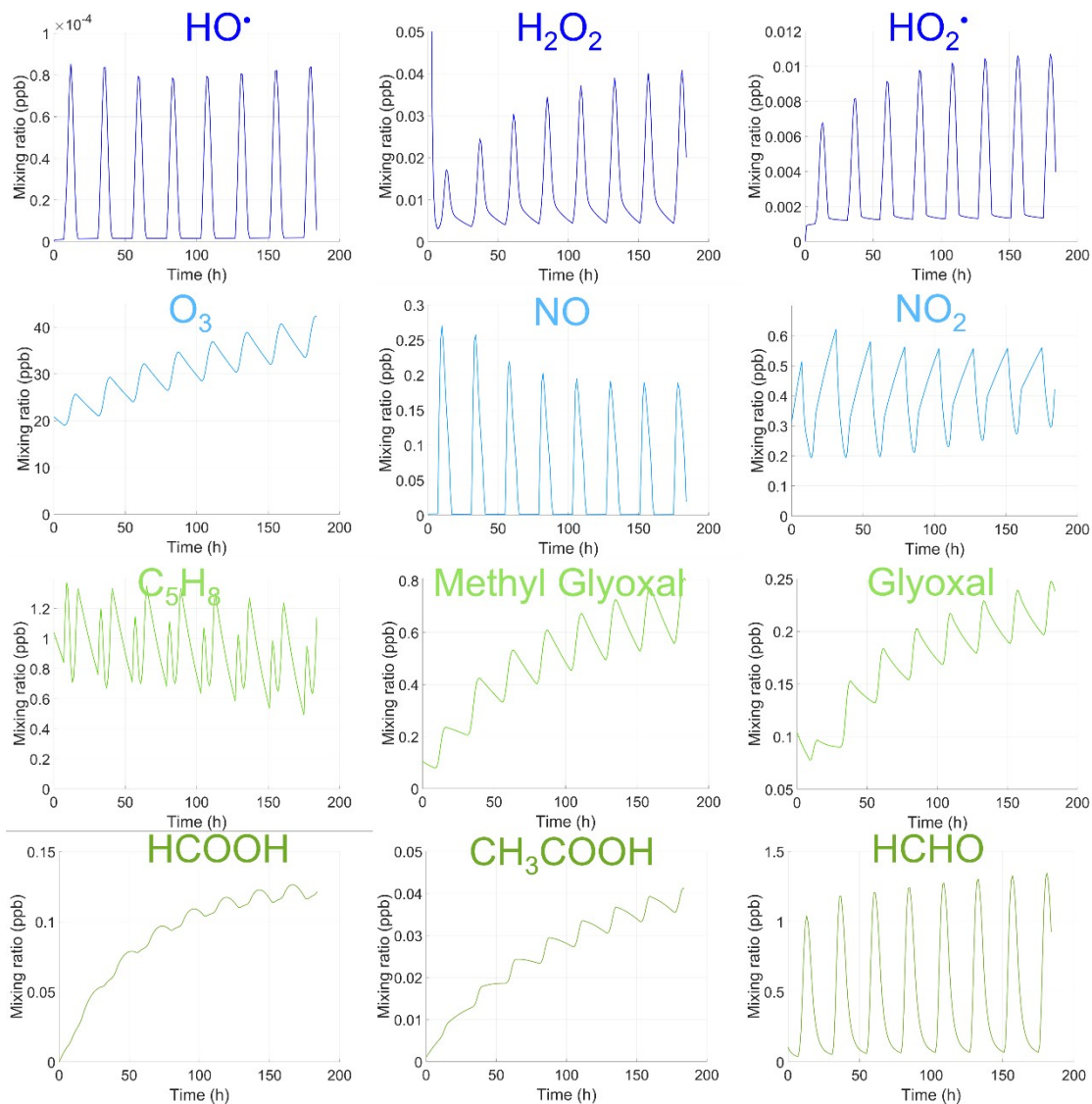


Figure SM2 : Time evolution of the concentration (ppb) of some selected gases during the spinup winter simulation.

Table SM4 : Mixing ratios of chemical species of interest simulated at the end of the spinup simulations. Daytime values are concentrations extracted the 7th day at 10:00 AM and nighttime values are concentrations extracted the 6th day at 10:00 PM.

Mixing ratio (ppb)	Summer		Winter	
	Night	Day	Night	Day
O₃	69	70	40	35
H₂O₂	1.7 10 ⁻²	0.20	1.3 10 ⁻²	1.9 10 ⁻²
NO	4.5 10 ⁻⁴	7.8 10 ⁻²	9.6 10 ⁻⁴	0.19
NO₂	0.46	0.24	0.42	0.39
SO₂	0.25	0.25	0.37	0.37
Formic acid	0.25	0.23	0.12	0.12
Formaldehyde	0.41	2.0	0.67	0.78
Acetic acid	0.42	0.33	3.9 10 ⁻²	3.9 10 ⁻²

S(7) d) Analysis of the simulated HOx variability with the environmental conditions

Mixing ratio (ppb / molec cm ⁻³)	Summer		Winter	
HO [•]	3.8 10 ⁻⁶ / 8.2 10 ⁴	1.8 10 ⁻⁴ / 3.9 10 ⁶	1.8 10 ⁻⁶ / 3.8 10 ⁴	6.9 10 ⁻⁵ / 1.5 10 ⁶
HO ₂ [•]	2.7 10 ⁻³ / 5.7 10 ⁷	3.4 10 ⁻² / 7.2 10 ⁸	1.4 10 ⁻³ / 3.1 10 ⁷	7.6 10 ⁻³ / 1.7 10 ⁸

For the summer day simulation, the HO[•] and HO₂[•] levels were realistic and comparable to measurements observed in low-NOx environments influenced by biogenic emissions. The review from Stones et al. (2012) presented a summary of measurements and model comparisons for HO[•] and HO₂[•] levels (see Table 3 in Stone et al., 2012) under these environmental conditions. For example, in Julich (Germany), during summer, the HO[•] and HO₂[•] levels were measured equal to 5–15 × 10⁶ molec cm⁻³ and 2–10 × 10⁸ molec cm⁻³, respectively.

Even if there is much less information on HOx levels during nighttime condition, some studies investigated the HOx diurnal variability as reported in the review from Stones et al. (2012). At night, the simulated HO[•] concentrations were two orders of magnitude than daytime values; this is consistent with previous studies (both modelling and experimental works) (Lu and Khalil, 1992; Sillman et al., 2002; Stones et al., 2012). For HO₂[•], the modelled nighttime concentrations presented a decrease by one order of magnitude compared to daytime concentrations. This is consistent with previous studies measurements performed during the BERLIOZ campaign in Germany (Platt et al., 2002) or during the PROPHET campaign in Michigan (US, Sillman et al., 2002).

For winter simulations, much less data on HOx levels were available. During the day, we simulated around 3 times lower HO[•] level and 4 times lower HO₂[•] levels in comparison to summer simulations. The actinic flux simulated in winter decreases by a factor 1.7 contributing to this lower HOx levels in winter vs summer. This range of decrease was consistent with some studies over semi-polluted or polluted areas (Ren et al., 2006; Kanaya et al., 2004; Heard et al., 2004).

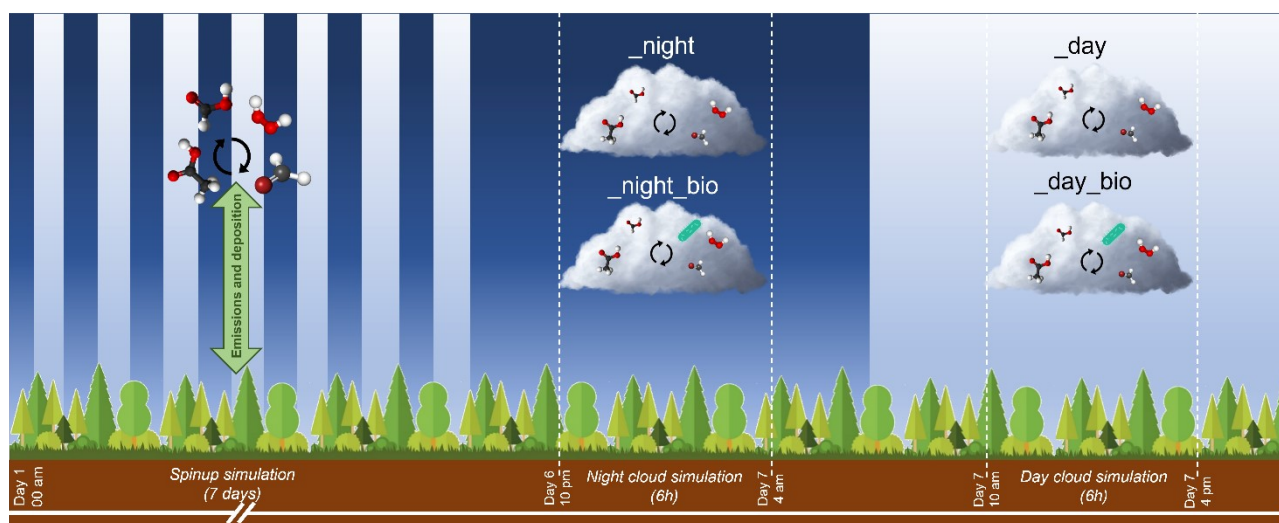
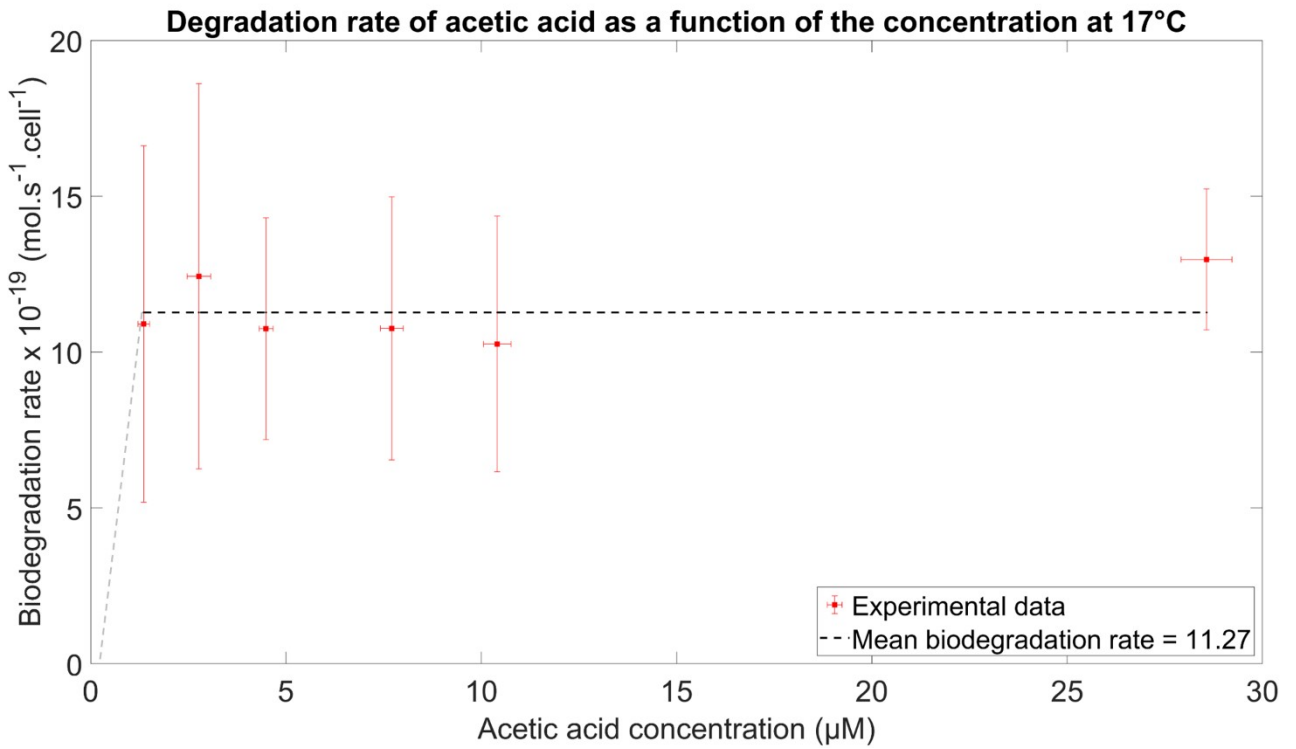
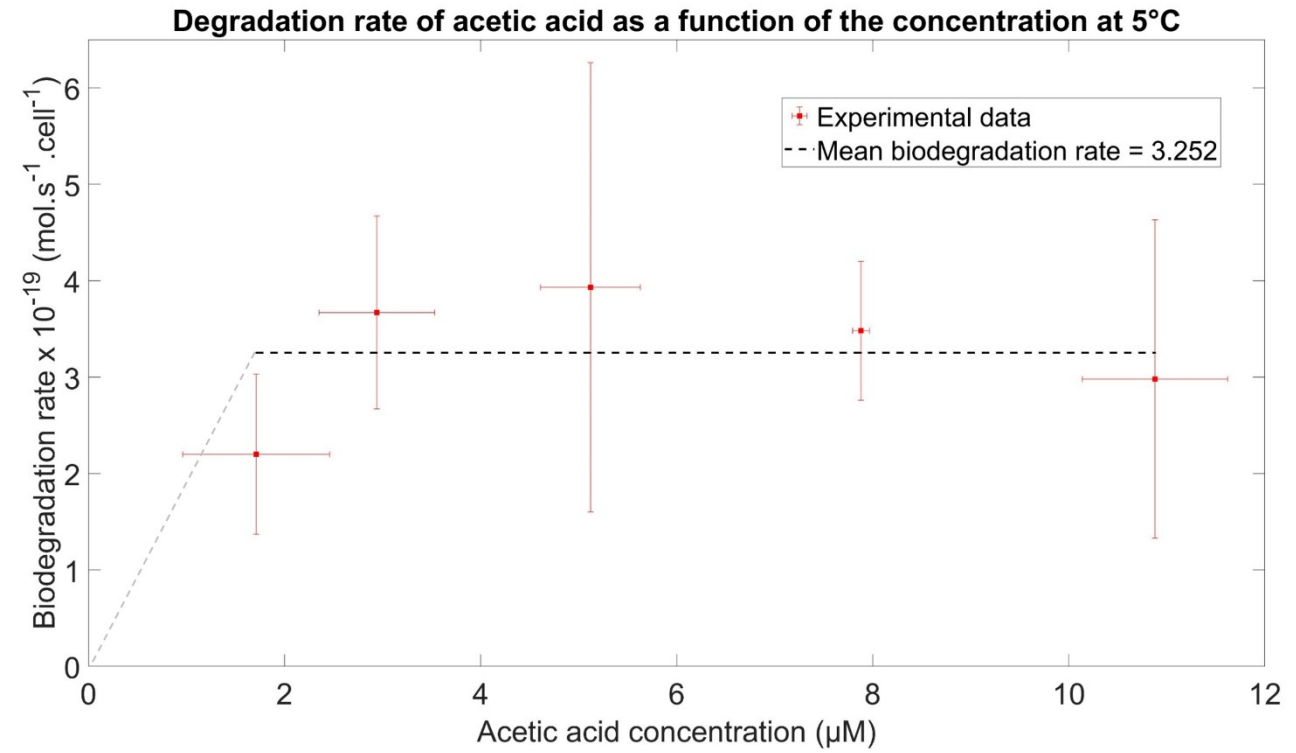
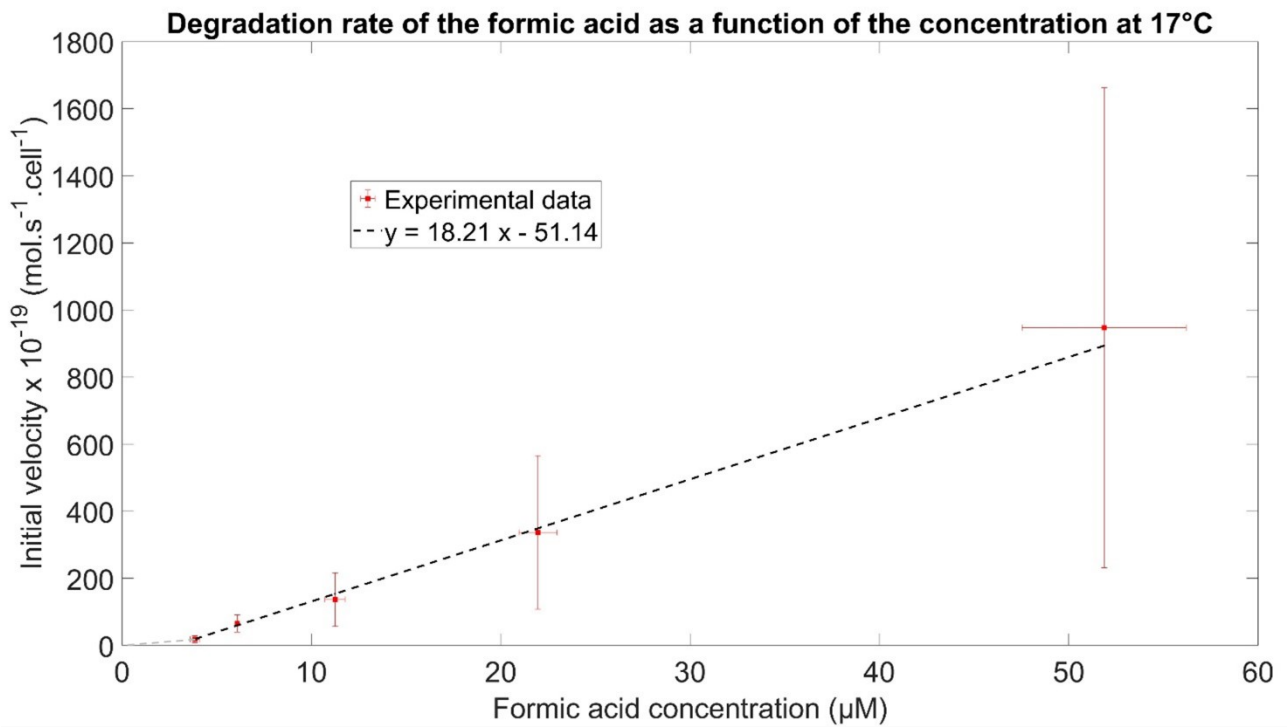
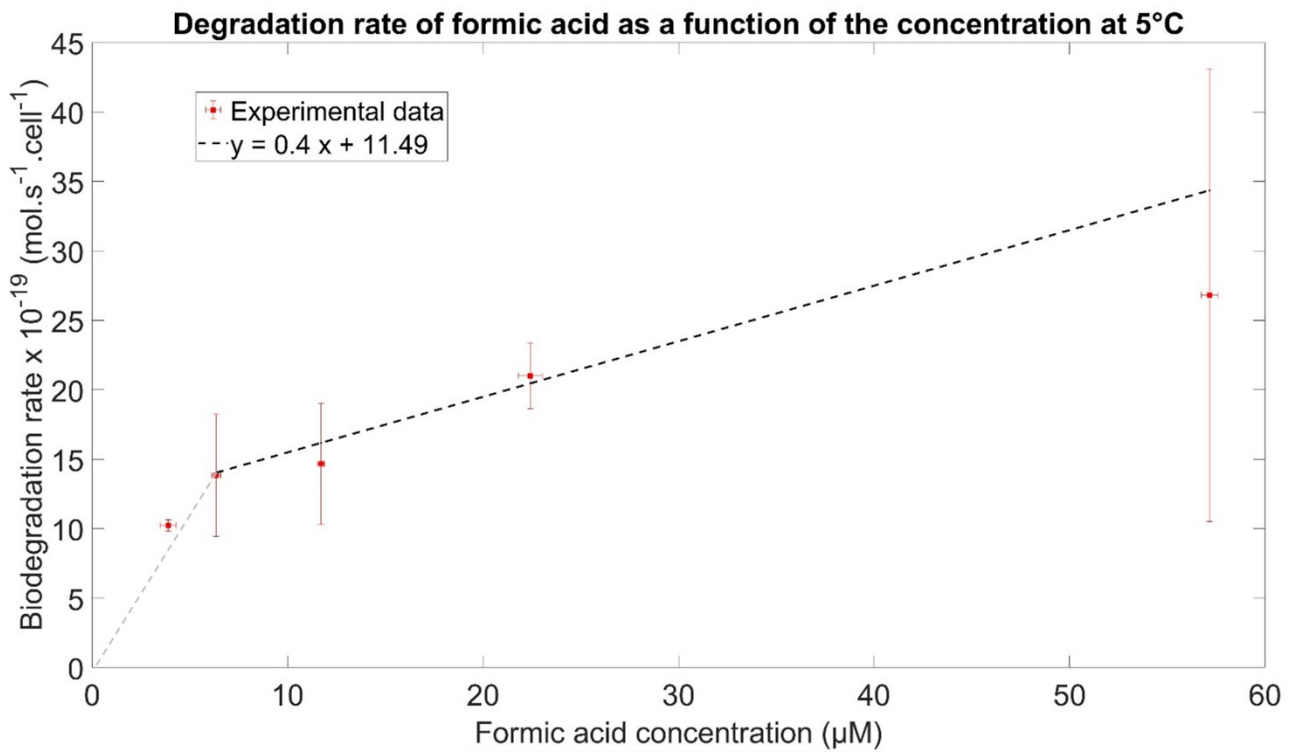


Figure SM3 : Scheme of the different simulations with the 7 day spinup simulation and the different cloud simulations : night and day cloud simulations, with or without microorganisms.

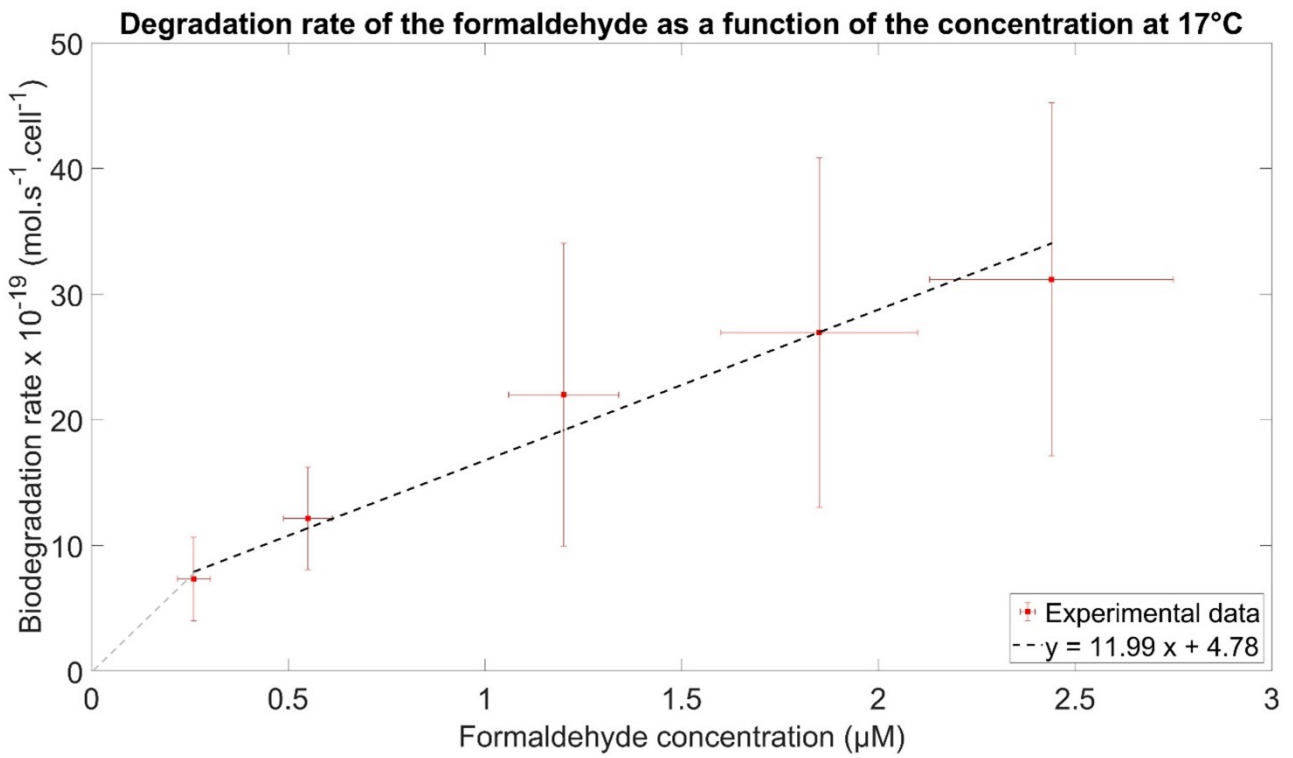
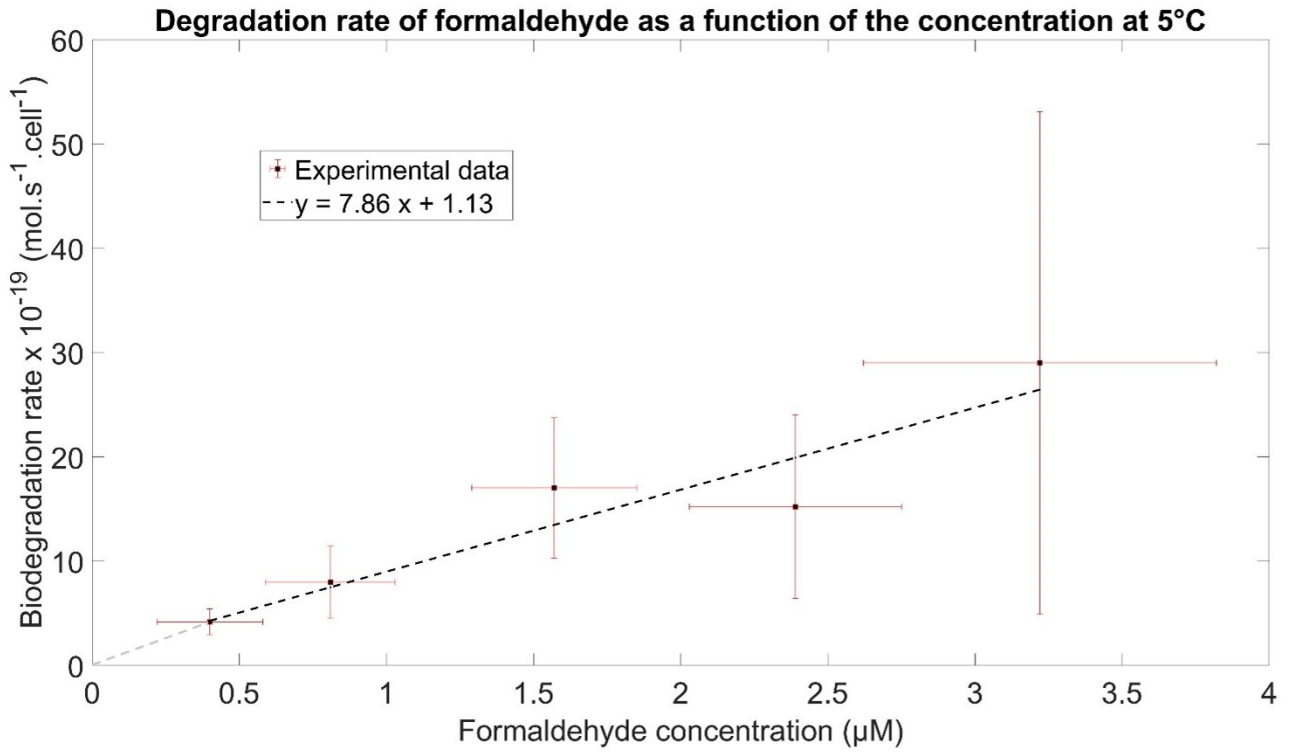
(S8) Linear fits of biodegradation rates



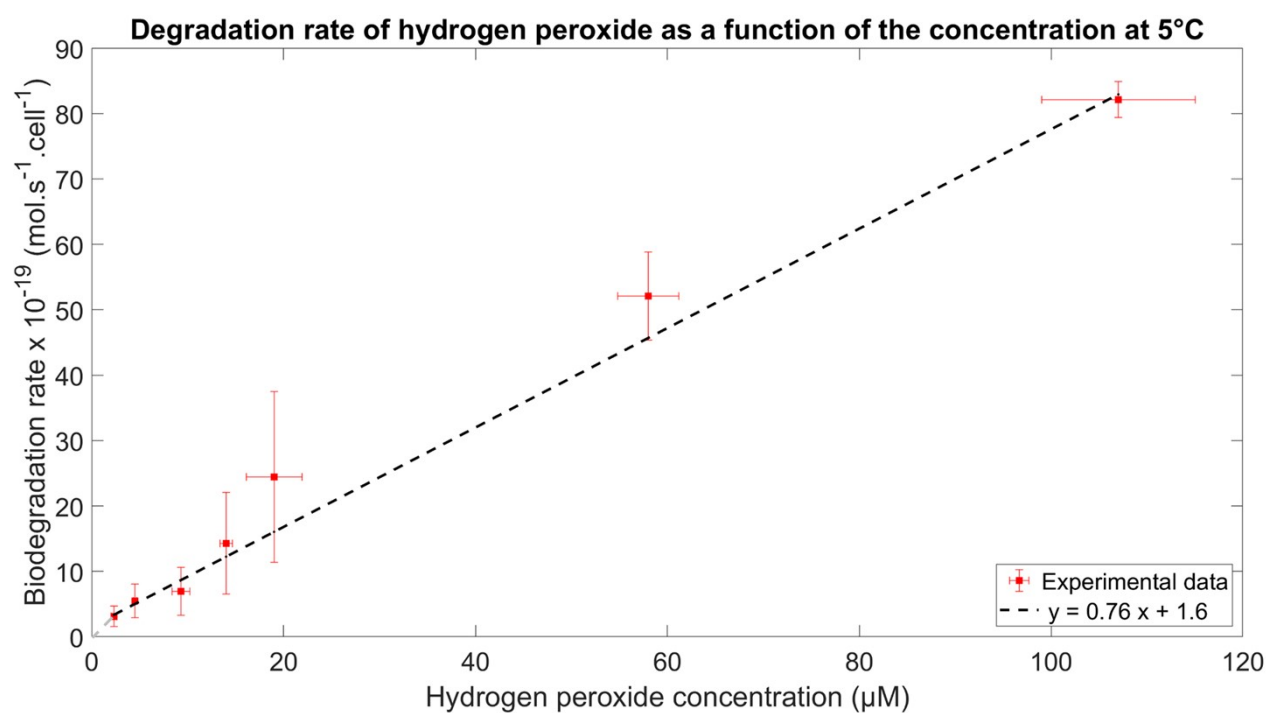
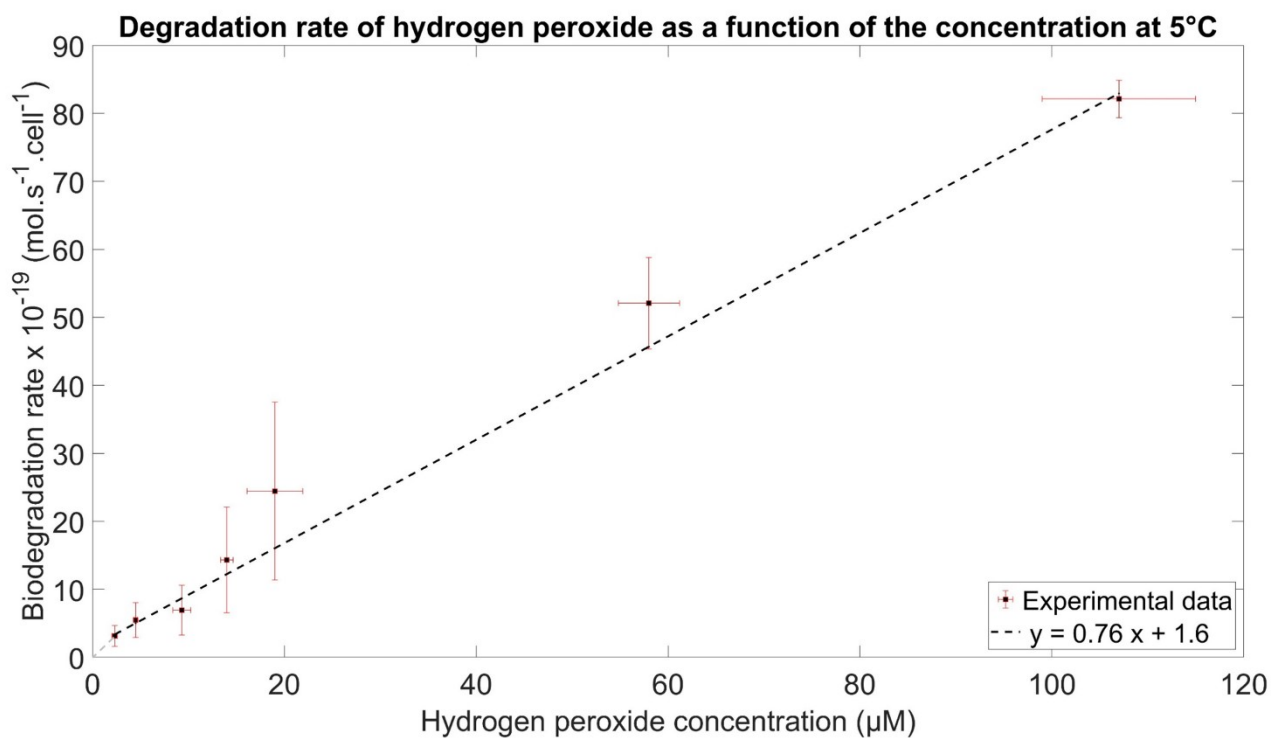
a)



b)



c)



d)

Figure SM4 : Acetic acid a), formic acid b), formaldehyde c) and hydrogen peroxide d) experimental biodegradation rate constants at 5 and 17°C as a function of the substrate concentration and the calculated slopes. The grey dashed line represents the linear fit between the origin and the last point of the calculated linear regression.

Linear regression

In the studied ranges of substrate concentrations, biodegradation kinetics were assimilated to linear function for each substrate and temperature. A linear regression was used allowing to calculate a slope that links the biodegradation rate and the substrate concentration. **Figure SM4** gives example of the slopes calculated from experimental data by the least squares method. Acetic acid biodegradation rate was assumed to be constant according to the data reported in **Figure SM4**. Biodegradation rates must obviously be equal to zero for a null substrate concentration. Thus, for concentration inferior to the lowest experimental substrate concentration, we use a linear fit between the origin (0;0) and the last point of the linear regression calculated above: this corresponds to the grey dashed line on **Figure SM4**.

Table SM5 reports the linear fits of the 4 selected species for the experimental ranges of concentration.

Table SM5 : Linear fits of the biodegradation rates of formic acid, acetic acid, formaldehyde, H_2O_2 at 17 and 5 °C as a function of the concentration.

	Formic acid	Acetic acid	Formaldehyde	H_2O_2
Rate at 17 °C	$y = 2.2 x$	$y = 110 x$	$y = 60 x$	$y = 3.2 x$
($\times 10^{-19} \text{ mol s}^{-1} \text{ cell}^{-1}$)	$y = 18 x - 51$	$y = 11$	$y = 12 x + 4.8$	$y = 1.1 x + 2.1$
Concentration range (μM)	0 – 4 4 – 52	0 – 0.1 0.1 – 30	0 – 0.1 0.1 – 5	0 – 1 1 – 120
Rate at 5 °C	$y = 3.1 x$	$y = 32 x$	$y = 19 x$	$y = 2.4 x$
($\times 10^{-19} \text{ mol s}^{-1} \text{ cell}^{-1}$)	$y = 0.40x + 11$	$y = 3.2$	$y = 7.9x + 1.1$	$0.76x + 1.6$
Concentration range (μM)	0 – 4 4 – 57	0 – 0.1 0.1 – 15	0 – 0.1 0.1 – 5	0 – 1 1 – 140

(S9) Aqueous concentrations of the HO[•] and HO₂[•]/O₂^{-•} radicals

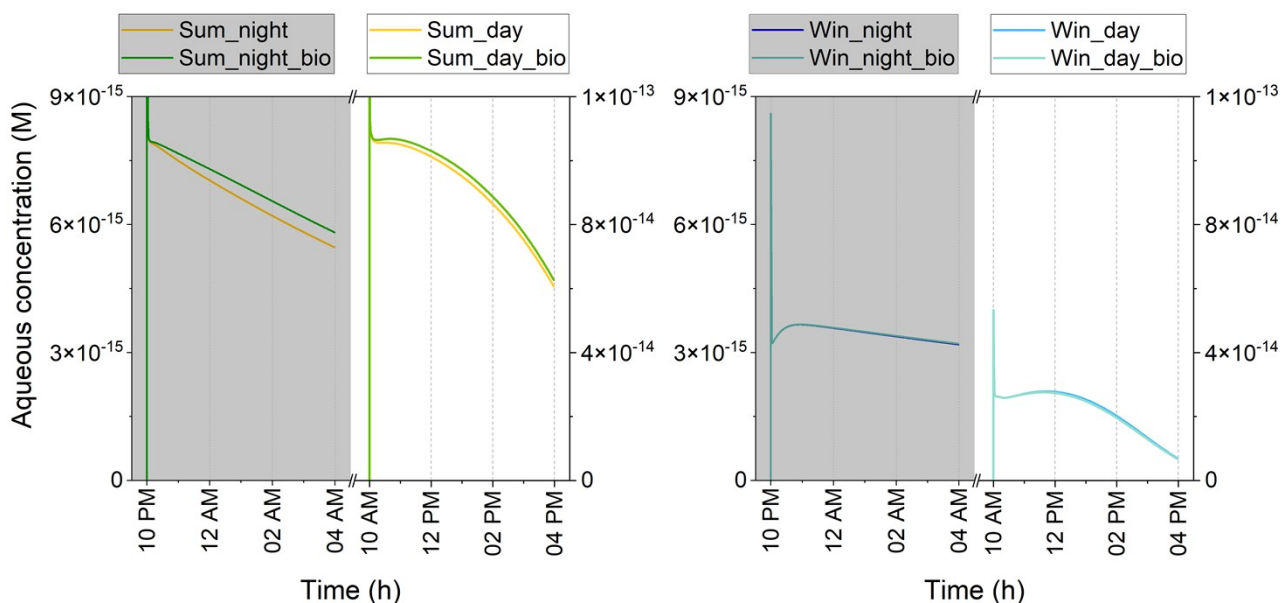


Figure SM5a: Time evolution of the concentrations in the aqueous phase of hydroxyl radical HO[•] for summer (left) and winter (right) simulations at night (grey box) and day. Each simulation is done with and without considering biodegradation.

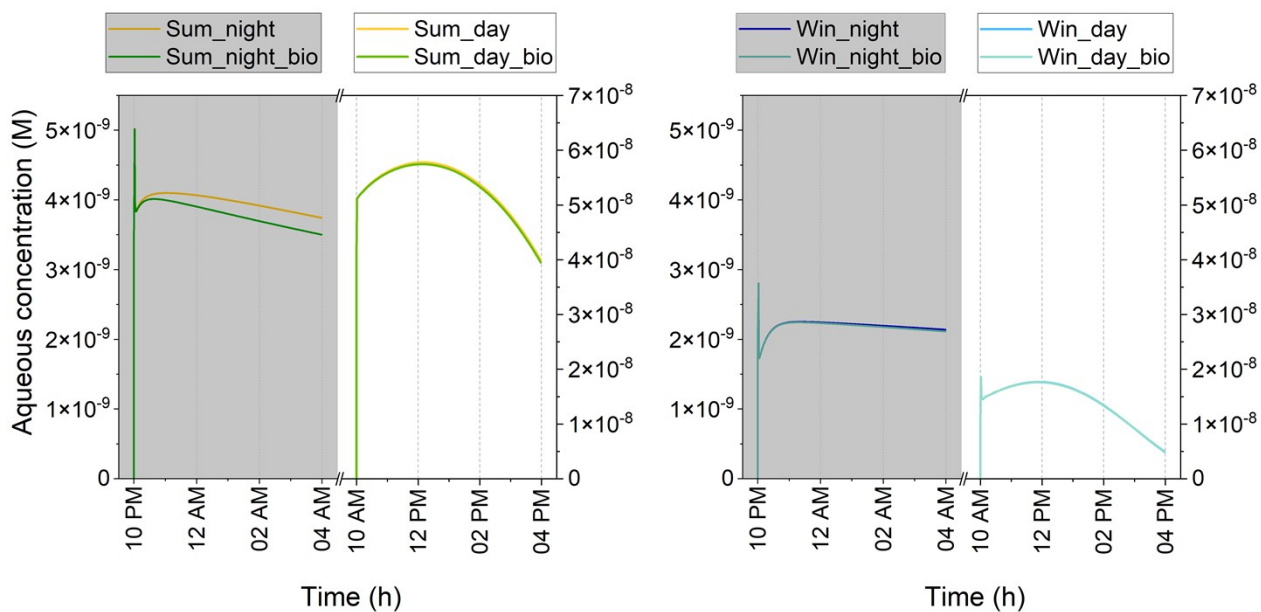


Figure SM5b: Time evolution of the concentrations in the aqueous phase of HO₂[•]/O₂^{-•} for summer (left) and winter (right) simulations at night (grey box) and day. Each simulation is done with and without considering biodegradation.

(S10) The different tests parameters

Table SM6: Conditions of the different test simulations (LWC, cell concentration and pH): chemical scenario, environmental parameters, microphysical properties, Dissolved Organic Carbon (DOC) concentration.

Conditions	Sum_day_ bio_LWC_1	Sum_day_ bio_LWC_9	Sum_day_ bio_cell_1	Sum_day_ bio_cell_12	Sum_day_ bio_pH_4.5
Chemical scenario	Summer	Summer	Summer	Summer	Summer
Date and time of simulation	June 21 st 10 AM - 4 PM				
Temperature (°C)	17	17	17	17	17
LWC (vol/vol)	1×10^{-7}	9×10^{-7}	3×10^{-7}	3×10^{-7}	3×10^{-7}
Droplet radius (μm)	10	10	10	10	10
DOC concentration (μM)	400	400	400	400	400
Cell concentration (cell L⁻¹)	$6.81 \cdot 10^7$	$6.81 \cdot 10^7$	$1.27 \cdot 10^7$	$12.35 \cdot 10^7$	$6.81 \cdot 10^7$
pH	5.5	5.5	5.5	5.5	4.5
Conditions	Sum_night_ bio_LWC_1	Sum_night_ bio_LWC_9	Sum_night_ bio_cell_1	Sum_night_ bio_cell_12	Sum_night_ bio_pH_4.5
Chemical scenario	Summer	Summer	Summer	Summer	Summer
Date and time of simulation	June 20 th 10 PM 21 st 4 AM				
Temperature (°C)	17	17	17	17	17
LWC (vol/vol)	1×10^{-7}	9×10^{-7}	3×10^{-7}	3×10^{-7}	3×10^{-7}
Droplet radius (μm)	10	10	10	10	10
DOC concentration (μM)	400	400	400	400	400
Cell concentration (cell L⁻¹)	$6.81 \cdot 10^7$	$6.81 \cdot 10^7$	$1.27 \cdot 10^7$	$12.35 \cdot 10^7$	$6.81 \cdot 10^7$
pH	5.5	5.5	5.5	5.5	4.5

(S11) Aqueous concentration and chemical budget of the four compounds for the different tests

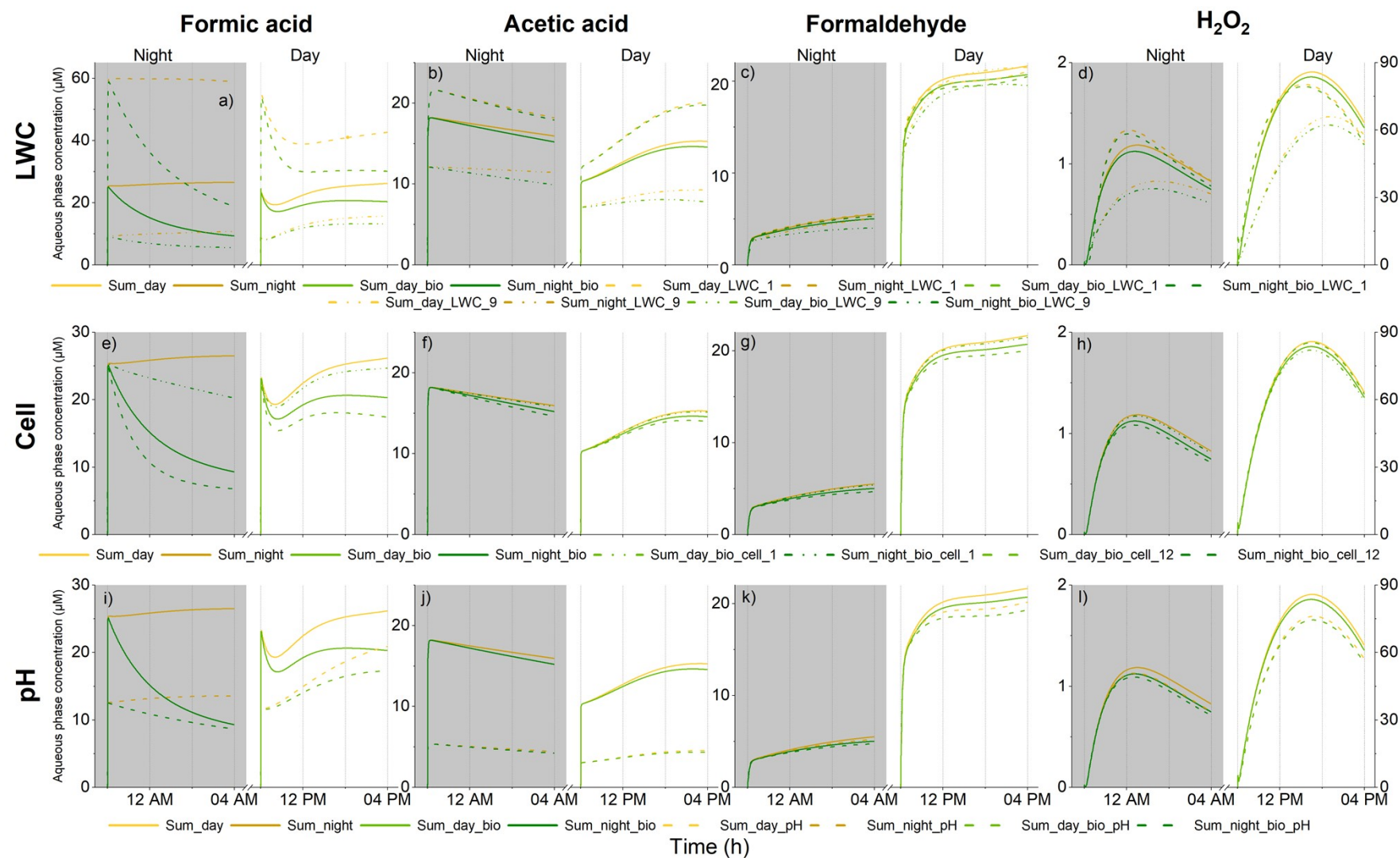


Figure SM6: Time evolution of the concentrations in the aqueous phase (μM) of formic and acetic acids, formaldehyde and hydrogen peroxide for the different tests (dotted and dashed lines) simulations at night (on the left) and day (on the right). Each simulation is compared to the reference simulation (solid lines).

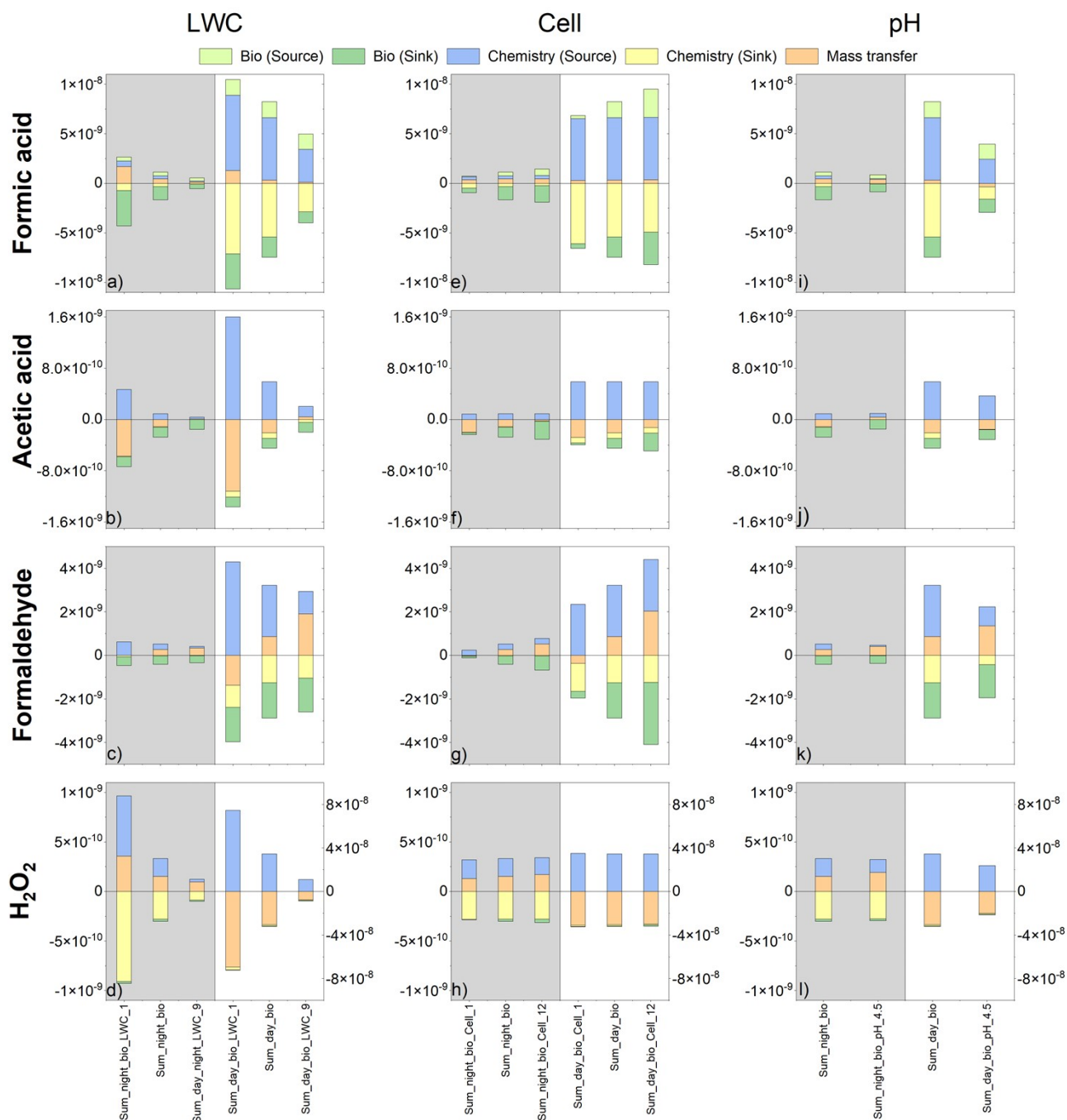


Figure SM7 : Chemical budget of formic and acetic acids, formaldehyde and H_2O_2 for the different tests (LWC, Cell concentration and pH variations) during summer simulations at day (white boxes) and night (gray boxes), with or without biodegradation. Production rates ($M s^{-1}$) (positive values) and destruction rates ($M s^{-1}$) (negative values) were integrated over the whole simulation (10 first minutes were excluded in these calculations). Chemical (blue) and biological (green) sources are presented as for the chemical (yellow) and biological (green) sinks. Mass transfer is presented in orange.

(S12) Total (aqueous + gas) concentration and chemical budget of acetic acid, formaldehyde and H₂O₂ for the different tests

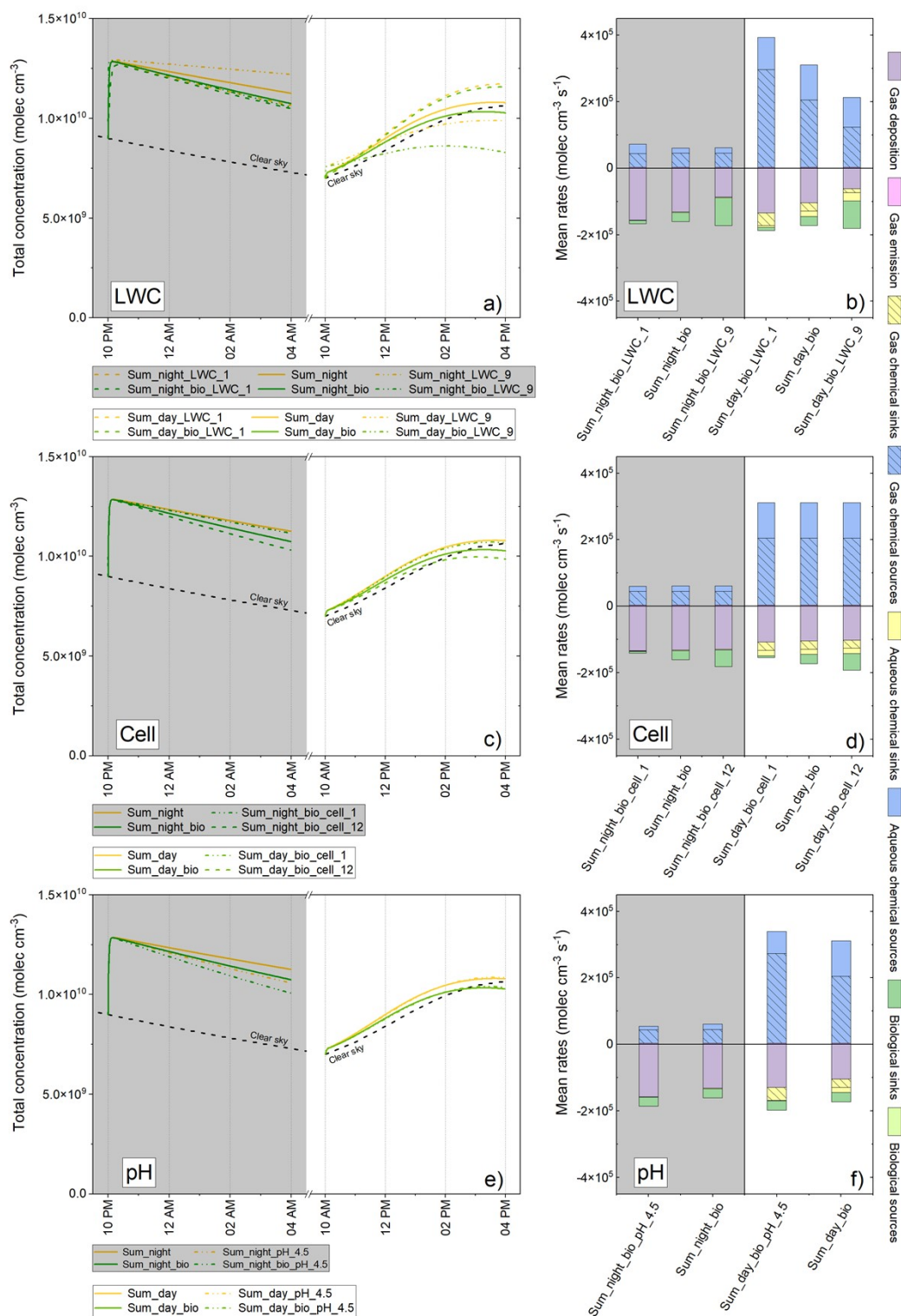


Figure SM8: Total concentrations (left) and multiphase chemical budgets (right) of acetic acid considering the LWC ("LWC_1": $1 \cdot 10^{-7}$ vol/vol; "LWC_9": $9 \cdot 10^{-7}$ vol/vol), the cell concentration ("cell_1": $1.27 \cdot 10^4$ cells mL⁻¹; "cell_12": $12.35 \cdot 10^4$ cells mL⁻¹) and the pH variations ("pH_4.5": 4.5). The total concentration is the sum (in molec.cm⁻³) of the aqueous and the gas phase concentrations of the different simulations with (green) and without (yellow) biodegradation. The total chemical budget considers the aqueous transformations: chemical sinks (yellow) and sources (blue) and biodegradation (green); and the gas phase transformations: the chemical sinks (hatched yellow) and sources (hatched blue) as well as the emission (pink) and deposition (purple) processes. The mass transfer is zero as it balances between the gas and the aqueous phases.

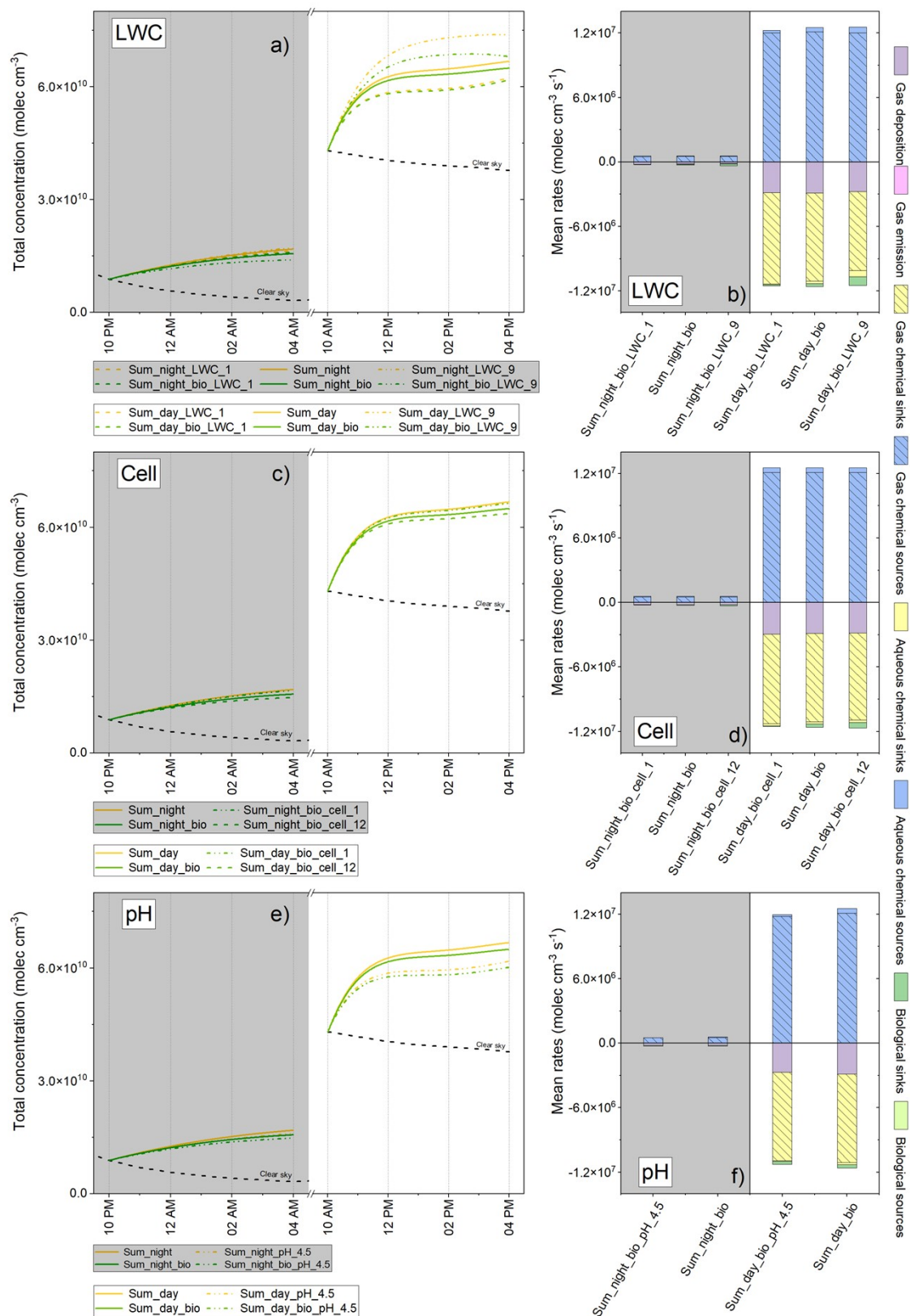


Figure SM9: Total concentrations (left) and multiphase chemical budgets (right) of formaldehyde considering the LWC ("LWC_1": $1 \cdot 10^{-7}$ vol/vol; "LWC_9": $9 \cdot 10^{-7}$ vol/vol), the cell concentration ("cell_1": $1.27 \cdot 10^4$ cells mL^{-1} ; "cell_12": $12.35 \cdot 10^4$ cells mL^{-1}) and the pH variations ("pH_4.5": 4.5). The total concentration is the sum (in $\text{molec} \cdot \text{cm}^{-3}$) of the aqueous and the gas phase concentrations of the different simulations with (green) and without (yellow) biodegradation. The total chemical budget considers the aqueous transformations: chemical sinks (yellow) and sources (blue) and biodegradation (green); and the gas phase transformations: the chemical sinks (hatched yellow) and sources (hatched blue) as well as the emission (pink) and deposition (purple) processes. The mass transfer is zero as it balances between the gas and the aqueous phases.

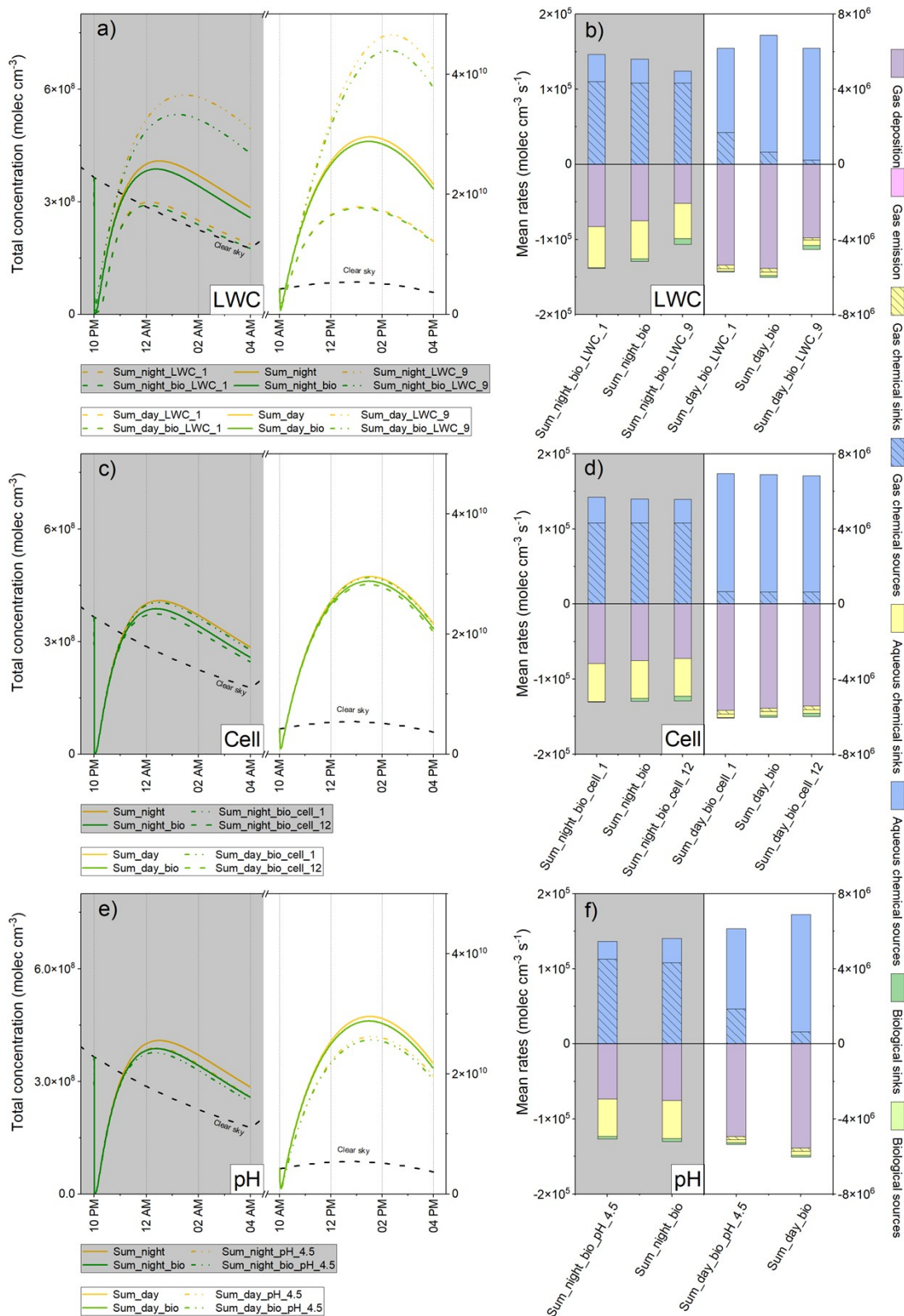


Figure SM10: Total concentrations (left) and multiphase chemical budgets (right) of H_2O_2 considering the LWC ("LWC_1": $1 \cdot 10^{-7}$ vol/vol; "LWC_9": $9 \cdot 10^{-7}$ vol/vol), the cell concentration ("cell_1": $1.27 \cdot 10^4$ cells mL^{-1} ; "cell_12": $12.35 \cdot 10^4$ cells mL^{-1}) and the pH variations ("pH_4.5": 4.5). The total concentration is the sum (in molec. cm^{-3}) of the aqueous and the gas phase concentrations of the different simulations with (green) and without (yellow) biodegradation. The total chemical budget considers the aqueous transformations: chemical sinks (yellow) and sources (blue) and biodegradation (green); and the gas phase transformations: the chemical sinks (hatched yellow) and sources (hatched blue) as well as the emission (pink) and deposition (purple) processes. The mass transfer is zero as it balances between the gas and the aqueous phases.

(S13) Henry's law constants

Table SM7: Henry's law constants (intrinsic and effective) of the 4 targeted species and main oxidants (HO^\bullet , HO_2^\bullet and O_3) (in M atm^{-1}) for the simulation conditions: temperature (5 and 17°C) and pH (5.5 and 4.5). Intrinsic Henry's law constants at 298K (and the temperature dependencies) are the ones considered in the cloud chemistry model (see Mouchel-Vallon et al., 2017).

Chemical species	H 298K	-Ea/R	Ka	Kh	H 278.15K	H 290.15K	H _{eff} 278.15K pH 5.5	H _{eff} 290.15K pH 5.5	H _{eff} 278.15K pH 4.5	H _{eff} 290.15K pH 4.5
HO^\bullet	$3.90 \cdot 10^1$	$6.01 \cdot 10^3$			$1.66 \cdot 10^2$	$6.80 \cdot 10^1$				
HO_2^\bullet	$6.90 \cdot 10^2$	$6.64 \cdot 10^3$	$1.6 \cdot 10^{-5}$		$3.43 \cdot 10^3$	$1.28 \cdot 10^3$	$2.08 \cdot 10^4$	$7.73 \cdot 10^3$	$5.16 \cdot 10^3$	$1.92 \cdot 10^3$
O_3	$1.03 \cdot 10^{-2}$	$2.83 \cdot 10^3$			$2.04 \cdot 10^{-2}$	$1.34 \cdot 10^{-2}$				
H_2O_2	$7.70 \cdot 10^4$	$7.31 \cdot 10^3$	$2.2 \cdot 10^{-12}$		$4.50 \cdot 10^5$	$1.51 \cdot 10^5$	$4.50 \cdot 10^5$	$1.51 \cdot 10^5$	$4.50 \cdot 10^5$	$1.51 \cdot 10^5$
Formaldehyde	2.48	$7.10 \cdot 10^3$		$1.30 \cdot 10^3$	$1.38 \cdot 10^1$	4.79	$1.79 \cdot 10^4$	$6.23 \cdot 10^3$	$1.79 \cdot 10^4$	$6.23 \cdot 10^3$
Formic acid	$8.90 \cdot 10^3$	$6.10 \cdot 10^3$	$1.80 \cdot 10^{-4}$		$3.88 \cdot 10^4$	$1.57 \cdot 10^4$	$2.25 \cdot 10^6$	$9.07 \cdot 10^5$	$2.60 \cdot 10^5$	$1.05 \cdot 10^5$
Acetic acid	$4.10 \cdot 10^3$	$6.20 \cdot 10^3$	$1.75 \cdot 10^{-5}$		$1.83 \cdot 10^4$	$7.28 \cdot 10^3$	$1.20 \cdot 10^5$	$4.76 \cdot 10^4$	$2.85 \cdot 10^4$	$1.13 \cdot 10^4$

(S14) Oxidative capacity of the aqueous phase for the different sensitivity tests (daytime)

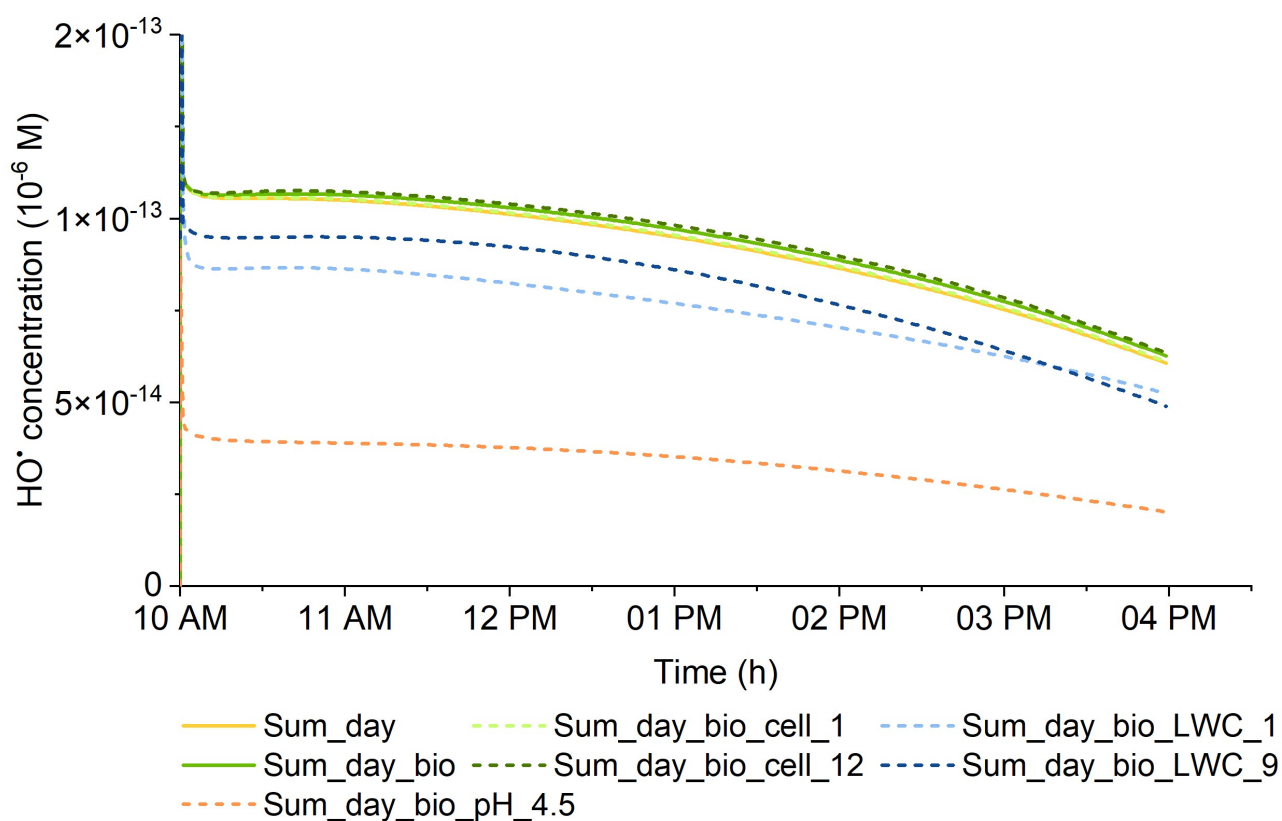


Figure SM11: Time evolution of the aqueous hydroxyl radical concentrations for the different sensitivity tests (daytime, summer). Solid lines represent the reference simulation (summer day with and without biodegradation). The dashed blue lines are the LWC tests, the green dashed lines are the cell concentration tests and the orange line is the pH test.

References

- Deguillaume, L., Charbouillot, T., Joly, M., Vaïtilingom, M., Parazols, M., Marinoni, A., Amato, P., Delort, A. M., Vinatier, V., Flossmann, A., Chaumerliac, N., Pichon, J. M., Houdier, S., Laj, P., Sellegri, K., Colomb, A., Brigante, M. and Mailhot, G.: Classification of clouds sampled at the puy de Dôme (France) based on 10 yr of monitoring of their physicochemical properties, *Atmospheric Chemistry and Physics*, 14(3), 1485–1506, 2014.
- Heard, D.E. et al.: High levels of the hydroxyl radical in the winter urban troposphere, *Geophysical Research Letter*, 31, L18112, 2004.
- Kanaya, Y. et al.: Urban photochemistry in central Tokyo: 1. Observed and modeled OH and HO₂ radical concentrations during the winter and summer of 2004, *Journal of Geophysical Research*, 112, D21312, 2004.
- Lazrus, A.L, Kok, G.L, Gitlin, S.N, Lind, J.A, McLaren S.E.: Automated fluorimetric method for hydrogen peroxide in atmospheric precipitation, *Analytical Chemistry*, 57(4), 917–922, 1985.
- Mouchel-Vallon, C., Deguillaume, L., Monod, A., Perroux, H., Rose, C., Ghigo, G., Long, Y., Leriche, M., Aumont, B., Patryl, L., Armand, P., and Chaumerliac, N.: CLEPS 1.0: A new protocol for cloud aqueous phase oxidation of VOC mechanisms, *Geoscientific Model Development*, 10, 1339–1362, 2017.
- Lu, Y., Khalil, K.: Model calculations of night-time atmospheric OH, *Tellus*, 44B, 106–113, 1992.
- Platt, U., Alicke, B., Dubois, R., et al.: Free radicals and fast photochemistry during BERLIOZ, *Journal of Atmospheric Chemistry*, 42, 359–394, 2002.
- Reasoner, D. J., Geldreich, E. E.: A new medium for the enumeration and subculture of bacteria from potable water. *Applied and Environmental Microbiology*, 49 (1), 1–7, 1985.
- Ren, X., et al.: Behavior of OH and HO₂ in the winter atmosphere in New York City, *Atmospheric Environment*, 40, 252–263, 2006.
- Sillman S., et al.: Loss of isoprene and sources of nighttime OH radicals at a rural site in the United States: Results from photochemical models, *Journal of Geophysical Research*, 107(D5), 2002.
- Stone, D., Whalley, L.K., Heard, D.E.: Tropospheric OH and HO₂ radicals: field measurements and model comparisons, *Chemical Society Reviews*, 41, 6348–6404, 2012.
- Vaïtilingom, M., Deguillaume, L., Vinatier, V., Sancelme, M., Amato, P., Chaumerliac, N. and Delort, A.-M.: Potential impact of microbial activity on the oxidant capacity and organic carbon budget in clouds, *PNAS*, 110(2), 559–564, 2013.
- Van der Heyden, Y., Nguyen Minh Nguyet, A., Detaevernier, M.R., Massart, D.L., Plaizier-Vercammen, J.: Simultaneous determination of ketoconazole and formaldehyde in a shampoo: liquid chromatography method development and validation, *Journal of Chromatography A*, 958 (1-2), 191–201, 2002.